



**HAL**  
open science

## **Extracellular Nucleotide Catabolism by the Group B Streptococcus Ectonucleotidase NudP Increases Bacterial Survival in Blood**

Arnaud Firon, Márcia Dinis, Bertrand Raynal, Claire Poyart, Patrick Trieu-Cuot, Pierre-Alexandre Kaminski

► **To cite this version:**

Arnaud Firon, Márcia Dinis, Bertrand Raynal, Claire Poyart, Patrick Trieu-Cuot, et al.. Extracellular Nucleotide Catabolism by the Group B Streptococcus Ectonucleotidase NudP Increases Bacterial Survival in Blood. *Journal of Biological Chemistry*, 2014, 289 (9), pp.5479-5489. 10.1074/jbc.M113.545632 . pasteur-01299774

**HAL Id: pasteur-01299774**

**<https://pasteur.hal.science/pasteur-01299774>**

Submitted on 8 Apr 2016

**HAL** is a multi-disciplinary open access archive for the deposit and dissemination of scientific research documents, whether they are published or not. The documents may come from teaching and research institutions in France or abroad, or from public or private research centers.

L'archive ouverte pluridisciplinaire **HAL**, est destinée au dépôt et à la diffusion de documents scientifiques de niveau recherche, publiés ou non, émanant des établissements d'enseignement et de recherche français ou étrangers, des laboratoires publics ou privés.

# Extracellular Nucleotide Catabolism by the Group B *Streptococcus* Ectonucleotidase NudP Increases Bacterial Survival in Blood\*

Received for publication, December 23, 2013, and in revised form, January 13, 2014. Published, JBC Papers in Press, January 15, 2014, DOI 10.1074/jbc.M113.545632

Arnaud Firon<sup>‡§</sup>, Marcia Dinis<sup>‡§</sup>, Bertrand Raynal<sup>¶</sup>, Claire Poyart<sup>||\*\*\*††</sup>, Patrick Trieu-Cuot<sup>‡§</sup>, and Pierre Alexandre Kaminski<sup>‡§1</sup>

From the Institut Pasteur, <sup>‡</sup>Unité de Biologie des Bactéries Pathogènes à Gram-Positif and <sup>¶</sup>Plateforme de Biophysique des Macromolécules et de leurs Interactions, F-75015 Paris, France, <sup>§</sup>CNRS, ERL3526, F-75015 Paris, France, <sup>||</sup>Institut Cochin, Université Sorbonne Paris Descartes, F-75014 Paris, France, <sup>\*\*</sup>INSERM, U1016, F-75014 Paris, France, and <sup>††</sup>Assistance Publique Hôpitaux de Paris, Service de Bactériologie, F-75014 Paris, France

**Background:** Ectonucleotidases regulate extracellular nucleotide concentration.

**Results:** The NudP ecto-5'-nucleotidase of *Streptococcus agalactiae* has specific substrate specificities necessary for survival in blood and organ colonization.

**Conclusion:** Extracellular nucleotide catabolism is involved in the control of Group B streptococcal pathogenesis.

**Significance:** Bacterial pathogens exploit different enzymatic specificities to subvert extracellular nucleotide signaling.

*Streptococcus agalactiae* (Group B *Streptococcus*) is a commensal of the human intestine and vagina of adult women but is the leading cause of invasive infection in neonates. This Gram-positive bacterium displays a set of virulence-associated surface proteins involved in the interaction with the host, such as adhesion to host cells, invasion of tissues, or subversion of the immune system. In this study, we characterized a cell wall-localized protein as an ecto-5'-nucleoside diphosphate phosphohydrolase (NudP) involved in the degradation of extracellular nucleotides which are central mediators of the immune response. Biochemical characterization of recombinant NudP revealed a Mn<sup>2+</sup>-dependent ecto-5'-nucleotidase activity on ribo- and deoxyribonucleoside 5'-mono- and 5'-diphosphates with a substrate specificity different from that of known orthologous enzymes. Deletion of the gene coding the housekeeping enzyme sortase A led to the release of NudP into the culture supernatant, confirming that this enzyme is anchored to the cell wall by its non-canonical LPXTN motif. The NudP ecto-5'-nucleotidase activity is reminiscent of the reactions performed by the mammalian ectonucleotidases CD39 and CD73 involved in regulating the extracellular level of ATP and adenosine. We further demonstrated that the absence of NudP activity decreases bacterial survival in mouse blood, a process dependent on extracellular adenosine. *In vivo* assays in animal models of infection showed that NudP activity is critical for virulence. These results demonstrate that Group B *Streptococcus* expresses a specific ecto-5'-nucleotidase necessary for its pathogenicity and highlight the diversity of reactions performed by this enzyme family. These results suggest that bacterial pathogens

have developed specialized strategies to subvert the mammalian immune response controlled by the extracellular nucleotide signaling pathways.

Pathogenic microorganisms have developed numerous strategies to resist and manipulate the host immune system to avoid recognition and killing. One of them relies on the perturbation of the host purinergic signaling pathway to control the balance between pro- and anti-inflammatory responses (1, 2). This purinergic pathway uses mainly extracellular adenosine triphosphate (eATP)<sup>2</sup> and extracellular adenosine (eAdo) as signaling effectors. In response to infection or cell damage, host cells secrete ATP (3, 4). eATP is a “danger” signal allowing the recruitment of the innate immune system and the autocrine activation of proinflammatory responses (3–8). In contrast, eAdo antagonizes the effect of eATP and is a very potent suppressor of proinflammatory responses (9, 10). eAdo and eATP are recognized by specific cell surface receptors of the P1 and P2 families regulating the balance between anti- and proinflammatory responses as well as numerous cell-cell communication processes and pathological conditions (7, 9–11).

The eATP/eAdo ratio is tightly regulated by ectonucleotidases expressed at the surface of host cells to avoid detrimental overactivation of the proinflammatory response by eATP (12, 13). In mammals, two main ectonucleotidases, CD39 and CD73, allow the sequential degradation of eATP to eAdo (12, 13). The CD39 enzyme is an ectonucleoside triphosphate diphosphohydrolase (ecto-NTPDase) that hydrolyzes the terminal phosphoryl group of nucleoside tri- and diphosphates

\* This work was supported by the Institut Pasteur, the CNRS, the French Government's Investissement d'Avenir program, Laboratoire d'Excellence “Integrative Biology of Emerging Infectious Diseases” Grant ANR-10-LABX-62-IBEID, and Fondation pour la Recherche Médicale Grant DEQ20130326538.

<sup>1</sup> To whom correspondence should be addressed: Inst. Pasteur, Dépt. de Microbiologie, Unité de Biologie des Bactéries Pathogènes à Gram-Positif, 25–28, rue du docteur Roux, F-75015 Paris, France. Tel.: 33-1-45-68-82-97; Fax: 33-1-45-68-84-04; E-mail: pierre-alexandre.kaminski@pasteur.fr.

<sup>2</sup> The abbreviations used are: eATP, extracellular adenosine triphosphate; eAdo, extracellular adenosine; NTPDase, nucleoside triphosphate diphosphohydrolase; GBS, Group B *Streptococcus*; TH, Todd Hewitt; Bis-Tris, 2-[bis(2-hydroxyethyl)amino]-2-(hydroxymethyl)propane-1,3-diol; SrtA, sortase A; SrtA\*, inactive sortase A; NudP, ecto-5'-nucleoside diphosphate phosphohydrolase; NudP\*, inactive NudP; rNudP, recombinant NudP; eN, ecto-5'-nucleotidase; UshA, UDP-sugar hydrolase.

## Specific Ecto-5'-nucleosidase Activity of *S. agalactiae*

**TABLE 1**  
Primers used in this study

Name	Sequence (5' to 3')	Feature <sup>a</sup>
NdP5	AAGGATCCATGGACCAAGTCGGCGTCCAAGTTATAGG	BamHI
NdP3	AGAAATTCCTTATTGTTTTGATTTTACAGTAGTGGAGTTTGATGGTTTTGC	EcoRI
483	TCATGAATTCGTCCTCAAGTTATAGCGGCTCAATG	EcoRI
337	CAAACCTTCATCAAAtgcacctgcACTAATGTGCCACTACTCAACA	AGA
338	AGTATGGCACATTAGGTgcaggtgcaTTTGATGAAGGTTTGGCAGA	AGA
484	TCATGGATCCGACAAGGTTTGGGATGTCTTTGG	BamHI
334	GTGAGAACTATTTTAAACAACC	
341	AACCTTCATCAAATTCATGGTT	
342	AACCTTCATCAAAtgcacctgc	AGA
340	ACTACTTTAGCTGAAGGGGTTTC	
184	AGTAGGTACCTAACATGGTACTGTGCAATTTTTTC	KpnI
303	cataaggaatgatgtccatattcaGCGAAATCATTTTTTATTGACGA	Δ
304	TCGTCAAATAAAAAATGATTTTCGCTgaatatggacaatcattccttatg	Δ
187	TCATAAGCTTATCAAGAATTGCAACGTATTATGAA	HindIII
188	ATCGCCATATTTTGTAGCTAATGTTTC	
189	TACCTGGGTGCTATTAAGTTTTTC	

<sup>a</sup> Features include restriction sites (underlined), mutations for AGA substitution (lowercase), and composite primers for chromosomal deletion (underlined lowercase).

(NTP and NDP) to nucleoside monophosphates (NMPs), and the unrelated CD73 enzyme is an ecto-5'-nucleotidase that catalyzes the hydrolysis of phosphate esterified at carbon 5' of the ribose and deoxyribose moieties of the NMP molecules to give the corresponding nucleoside (12).

Recently, functional homologues of CD39 have been identified in a number of microbial human pathogens (14), such as *Legionella pneumophila* (15–17), and proteins belonging to the CD73 family of ecto-5'-nucleotidase have been identified in *Staphylococcus aureus*, *Bacillus anthracis*, and *Streptococcus sanguinis* (18–21). Inactivation of these bacterial ectonucleotidases impairs virulence but not viability, suggesting that their selective inhibition might be a new therapeutic strategy. Of note, each bacterial nucleotidase harbors specific enzymatic activity compared with the related mammalian enzymes. For instance, the *S. aureus* AdsA hydrolyzes AMP, ADP, and ATP in contrast to the related mammalian CD73 5'-nucleotidase, which hydrolyzes only AMP (12, 19).

In this study, we identified and characterized a putative ectonucleotidase of *Streptococcus agalactiae*, also known as Group B *Streptococcus* (GBS). GBS is a Gram-positive commensal bacterium of the human intestine and of the vagina of 10–30% of healthy women. However, GBS may turn into a deadly pathogen in neonates and is the leading cause of neonatal pneumonia, septicemia, and meningitis in high income countries (22–24). Despite early antimicrobial treatment and improvement in neonatal intensive care, up to 10% of neonatal GBS infections are lethal, and 25–35% of surviving infants with meningitis experience permanent neurological sequelae (25).

Innate immunity against GBS represents the critical first-line barrier of host defenses as newborns have a naïve adaptive immune system (26–28). Central to this response are host phagocytic cells, including neutrophils and macrophages, whose activities are dependent on the eATP/eAdo ratio. Moreover, innate immunity of the newborns appears polarized toward an anti-inflammatory response due, at least in part, to an elevated eAdo concentration in the cord and neonate bloods (27–30). Given the putative large effects of the eATP/eAdo ratio on the control of bacterial infections, we studied the GBS ecto-5'-nucleoside diphosphate phosphohydrolase (NudP), which was previously identified as one of the major immunoreactive proteins during bovine mastitis (31). We show that NudP

hydrolyzes ribo- and deoxyribonucleoside 5'-di- and -monophosphates but not 5'-triphosphates and is localized at the GBS surface. We demonstrate that inactivation of the NudP enzymatic activity increases the clearance of GBS by blood cells, a process dependent on eAdo. However, the loss of NudP activity impacts bacterial virulence and organ colonization in animal models of infection. We conclude that NudP ectonucleotidase activity is involved in the degradation of extracellular nucleotides and subverts the host immune defenses in favor of bacterial survival.

### EXPERIMENTAL PROCEDURES

**Bacterial Strains and Growth Conditions**—GBS strains used in this study are derivatives of NEM316, a fully sequenced ST-23 serotype III clinical isolate (RefSeq accession number NC\_004368.1) (32). GBS was cultured at 37 °C in Todd Hewitt (TH) broth (Difco, BD Biosciences) without agitation and on TH agar or Columbia agar supplemented with 10% horse blood (BioMerieux). *Escherichia coli* DH5α (Invitrogen), BLR (a *recA* derivative of BL21), and XL1 Blue (Stratagene) were grown in Luria-Bertani broth (LB) medium. When specified, antibiotics were used at the following concentrations: for *E. coli*, ampicillin, 100 μg/ml; erythromycin, 150 μg/ml; kanamycin, 25 μg/ml; for GBS, erythromycin, 10 μg/ml; kanamycin, 1000 μg/ml.

**Cloning and Purification of Recombinant NudP (rNudP)**—rNudP (residues 28–656) was produced by first cloning a high fidelity PCR product (Phusion DNA polymerase, Thermo Scientific) obtained using GBS NEM316 genomic DNA as template and primers NdP5 and NdP3 (all primers used in this study are listed in Table 1). The resulting BamHI-EcoRI digestion product was cloned into the pMESS plasmid (a gift of J.-M. Betton, Institut Pasteur), a pMalc-p2x (New England Biolabs) derivative containing the signal sequence of *MalE* for targeting the recombinant protein into the periplasm. After Sanger sequencing (GATC Biotech), the resulting pMESS\_rNudP plasmid was transformed into *E. coli* BLR cells with ampicillin selection.

Large scale preparations of periplasmic proteins were performed as described (33). Briefly, overnight culture of BLR + pMESS\_rNudP was diluted 100 times in 2 liters of LB medium supplemented with ampicillin and incubated at 30 °C. When the cultures reached the exponential phase ( $A_{600} = 0.6$ ), expres-

sion of rNudP was induced for 3 h by adding 1 mM isopropyl 1-thio- $\beta$ -D-galactopyranoside. Cells were harvested (5000 rpm, 10 min, 4 °C), resuspended in ice-cold TSE (25 mM Tris-HCl, pH 7, 20% saccharose, 1 mM EDTA), centrifuged (9000 rpm, 10 min, 4 °C), resuspended in ice-cold H<sub>2</sub>O, and centrifuged (12,000 rpm, 10 min, 4 °C), and the periplasmic proteins were finally precipitated with ammonium sulfate at 4 °C.

For rNudP purification, the precipitated proteins were dialyzed (Spectra/Por membrane cutoff, 6–8 kDa; Spectrum Laboratories, Inc.) against 50 mM Bis-Tris, pH 7 at 4 °C. Chromatographic purification was performed with HiTrap QHP columns using a 0–30% gradient of 1 M NaCl. Fractions containing rNudP were pooled and concentrated by ammonium sulfate precipitation. The proteins were resuspended in 50 mM Bis-Tris, pH 7, NaCl 100 mM and further purified by gel filtration (HiLoad 16/60 Superdex 200, GE Healthcare) with a flow rate of 1 ml/min. Protein concentrations were determined by UV absorption at 280 nm.

**Analytical Ultracentrifugation**—Sedimentation velocity experiments were carried out at 20 °C in an XL-I analytical ultracentrifuge (Beckman Coulter). Samples were spun using an An60Ti rotor and 12-mm double sector epoxy centerpieces. The partial specific volume of NudP (0.738 ml·g<sup>-1</sup>) was estimated from their amino acid sequences using the software Sednterp. The same software was used to estimate the buffer viscosity ( $\eta = 1.027$  centipoises) and density ( $\rho = 1.004$  g·ml<sup>-1</sup>). rNudP (400  $\mu$ l at 5, 9, and 22  $\mu$ M) was spun at 42,000 rpm, and absorbance profiles were recorded every 5 min. Sedimentation coefficient distributions,  $c(s)$ , were determined using the software Sedfit 14.1 (34). Sedimentation coefficients were extrapolated to zero concentration by linear regression, and values are presented for standard conditions (in water at 20 °C).

**Enzymatic Activity Assays**—Phosphatase activity was assayed by measuring the release of inorganic phosphate ( $P_i$ ) using the malachite green reagent following the manufacturer's recommendations (Biomol Green, Enzo Life Sciences). The reaction was carried out at 37 °C in 50 mM Bis-Tris adjusted to different pH values (between 5 and 8.9) containing various concentrations of nucleotides (from 10 to 500  $\mu$ M), cofactors, and a 1.5 nM concentration of the rNudP enzyme. After stopping the reaction with 1 ml of Biomol Green reagent, samples were incubated at room temperature for 20–30 min to allow development of the green color.  $P_i$  concentrations were determined by spectrophotometric absorbance measurements at 620 nm against a standard  $P_i$  curve.

Substrate degradation and product formation were followed by rapid resolution high performance liquid chromatography (HPLC) using a reverse-phase column (Agilent ZORBAX Eclipse XDB-C18, 2.1  $\times$  50 mm, 1.8  $\mu$ m). Enzymatic reactions were performed at 37 °C in 50 mM Bis-Tris, pH 7.5 containing 5 mM MnCl<sub>2</sub>, 100–200  $\mu$ M substrates (NTP, NDP, and NMP from Sigma), and 1.5 nM rNudP or rNudP\* or 0.1  $\mu$ g of cell wall extracts (see below for NudP\* mutagenesis and cell wall preparation). Products of the reactions were analyzed every 7 min by rapid resolution HPLC with a flow rate of 0.25 ml/min and a linear gradient of 1–12% CH<sub>3</sub>CN (2–13% CH<sub>3</sub>CN or 1–90% CH<sub>3</sub>CN) in 20 mM triethylammonium acetate buffer, pH 7.5.

The low resolution mass spectra were obtained by LC/MS (Agilent 1200 series LC with 6120 MS single quadrupole system) using an atmospheric electrospray ionization system.

**NudP Mutagenesis**—The conserved NudP motif NHE (residues 126–128) was changed to AGA (alanine-glycine-alanine) using a splicing by overlap-extension method as described previously with slight modifications (35, 36). Briefly, two  $\sim$ 280-bp PCR products flanking the chromosomal NHE region to be replaced were amplified with oligonucleotides containing the desired substitution (left product, primers 483 + 337; right product, primers 338 + 484). The two PCR products were purified, mixed, denatured, annealed, and then used as template for a second PCR with the external primers 483 + 484. The resulting 560-bp product was cloned after EcoRI-BamHI digestion into the thermosensitive shuttle plasmid pG1 to give the pG+NudP\* construct propagated into XL1 Blue *E. coli* (Stratagene) with kanamycin or erythromycin selection.

After Sanger sequencing (GATC Biotech) of the insert, plasmids were introduced in NEM316 by electroporation. GBS transformants were selected on erythromycin at 30 °C for 24–48 h to allow episomal replication of the pG+NudP\* plasmid. To select for pG+NudP\* chromosomal integration at the *nudP* locus, isolated transformants were plated and further isolated on erythromycin at 37 °C for 24–48 h. Isolated colonies with a stable integration by a single crossover of the pG+NudP\* plasmid into the chromosome at the *nudP* locus, referred to as integrants, were serially replicated (10<sup>-4</sup> dilution) two times a day in TH broth at 30 °C without erythromycin. An aliquot of each culture was spread on Columbia agar + 10% horse blood and cultured at 37 °C, and isolated colonies were tested for their resistance/susceptibility to erythromycin on TH agar at 37 °C by replica plating in a 96-well format. Erythromycin-sensitive colonies have lost the plasmid after a second crossover, leaving the wild-type (WT) *nudP* sequence or the *nudP*\* mutation. From the same parental integrant, analytical PCR was carried out to discriminate between WTbk (“WT back sequence”) and *nudP*\* mutants with primers 334 + 341 (=positive PCR product for a WT sequence) and primers 334 + 342 (=positive PCR product for a *nudP*\* sequence). Isogenic WTbk and *nudP*\* mutants were further confirmed by Sanger sequencing of PCR products (Phusion) of the *nudP* locus with primers 334 + 340 designed to anneal outside the genomic region used for the construction of the substitution cassette. Genomic DNA of the *nudP*\* mutant was further used to clone and express in *E. coli* the mutated rNudP\* protein after amplification with the primers NdP5 + NdP3 as described above for the WT rNudP allele.

***nudP* Chromosomal Deletion**—To confirm the specificity of antibodies made against NudP, we constructed a  $\Delta$ *nudP* deletion mutant in the NEM316 WT strain. The deletion construct was designed to delete 2110 bp of chromosomal DNA, starting from –125 bp of the *nudP* start codon and including 1985 bp of the 2073-bp *nudP* ORF, using a splicing by overlap-extension method as described above with primers 184 + 303 and primers 304 + 187. The second PCR product was obtained using the external primers 184 + 187, digested by KpnI and HindIII, and cloned into the thermosensitive shuttle plasmid pG1 to give the pG+ $\Delta$ *nudP* construct. After GBS transformation with pG+ $\Delta$ *nudP* (erythromycin, 30 °C) and selection of chromo-

## Specific Ecto-5'-nucleosidase Activity of *S. agalactiae*

somal integrants (erythromycin, 37 °C), we selected  $\Delta nudP$  mutant by screening erythromycin-sensitive colonies obtained after five subcultures at 30 °C by PCR with primers 188 + 189. Sanger sequencing was performed to confirm the deletion of the *nudP* genomic region. To confirm the NudP cell wall anchorage, we used the previously described inactive sortase A (SrtA\*) mutant obtained in an NEM316 WT background (37).

**NudP Immunodetection**—Cell surface and secreted proteins of GBS were prepared as described previously (38) from 50-ml midexponential growth cultures ( $A_{600} = 0.6$ ) at 37 °C in TH broth buffered with 100 mM Hepes. Cells were centrifuged; washed once in 50 mM Tris-HCl, pH 7.3; resuspended in 1 ml of osmoprotective buffer (50 mM Tris-HCl, pH 7.3, 20% sucrose, Roche Applied Science Complete protease inhibitors) supplemented with 175 units/ml mutanolysin (Sigma-Aldrich); and incubated for 90 min at 37 °C under constant gentle agitation. After centrifugation (13,500 rpm, 15 min, 4 °C), supernatants containing the cell wall proteins were used for the enzyme activity assays or for NudP immunodetection after SDS-PAGE or were kept frozen at -20 °C for further analysis.

For analysis of secreted proteins, supernatants from the same 50-ml cultures were additionally filtered (Millipore filter; pore size, 0.25  $\mu\text{m}$ ) to eliminate residual cells. Secreted proteins were precipitated with trichloroacetic acid (TCA; Sigma) overnight at 4 °C, centrifuged (4000 rpm, 30 min, 4 °C), washed with acetone (Sigma), centrifuged (4000 rpm, 30 min, 4 °C), and finally concentrated 100 times in 500  $\mu\text{l}$  of PBS with NaOH (5 mM) to neutralize TCA.

For NudP immunodetection, rabbit-specific polyclonal antibodies directed against rNudP were obtained from Covalab. Immunoglobulins were purified from total serum with protein A (Covalab) follow by an affinity purification step with immobilized rNudP on columns following the manufacturer's instructions (AminoLink coupling resin and immobilization kit, Thermo Scientific). Total proteins were quantified by the BSA method (Thermo Scientific), and the equivalent of secreted and cell wall proteins from  $10^8$  bacterial cells was used for NudP immunodetection. SDS-PAGE (Bis-Tris Criterion XT 4–12% gradient gels, Bio-Rad), protein transfer onto nitrocellulose membranes (Hybond-C, Amersham Biosciences), and chemiluminescence detection (Western Pico chemiluminescence, Thermo Scientific) with horseradish peroxidase (HRP)-coupled anti-rabbit secondary antibodies (Zymed Laboratories Inc.) were done following the manufacturers' instructions.

**GBS Survival in Blood**—Animal experiments were performed at the Institut Pasteur animal husbandries (Paris, France) in accordance with the policies of the European Union guidelines for the handling of laboratory animals with additional protocols approval by the Institut Pasteur animal care and use committee (Number 04.118). Whole blood was collected by cardiac puncture of 5-week-old female BALB/c mice into tubes containing anticoagulant (Vacuette Premium, Lithium Heparin Ridged, Greiner Bio-One). The blood of 10 mice was pooled and kept for a maximum of 15 min before use.

Overnight cultures of GBS strains were diluted 1:100 into fresh TH broth and grown at 37 °C to midexponential phase (OD = 0.6). Bacterial cells were centrifuged, washed twice, and

diluted in PBS to yield  $10^8$  cfu/ml. A total of  $5 \times 10^7$  bacteria (50  $\mu\text{l}$ ) were mixed with mouse blood (250  $\mu\text{l}$ ) supplemented with mock (PBS), adenosine, or guanosine (Sigma) at 150  $\mu\text{M}$  final concentration. Bacteria in blood solutions were incubated at 37 °C under constant gentle agitation. Time-dependent bacterial survival was quantified by plating aliquots on TH agar and enumeration of cfu after 24-h incubation. The percentage of GBS survival was calculated as follows:  $100 \times (\text{cfu after incubation with blood cells/cfu at time 0})$ . Statistical analysis (unpaired *t* test) from two independent experiments in duplicate was performed with Prism (GraphPad).

**In Vivo Virulence Studies**—Neonatal Sprague-Dawley rat pups (2 days old; Janvier, France) were randomized in groups of 10. Animals were inoculated intraperitoneally with a solution containing a total of  $5 \times 10^6$  bacteria in 100  $\mu\text{l}$  of PBS prepared from a midexponential phase (OD = 0.6) culture. Mortality curves were determined from two independent experiments by following animal survival over a 5-day period.

Adult animal infections were performed with 5-week-old female BALB/c mice (Charles River). Mice were injected intravenously via the tail vein with  $5 \times 10^7$  bacteria harvested in late exponential phase (OD = 0.6), washed in PBS, and resuspended in 500  $\mu\text{l}$ . At 24 and 48 h after injection, mouse groups (eight by bacterial strains) were sacrificed. Macroscopic observation of the different organs showed no significant difference between the different groups of animals, and bacterial counts in blood and homogenates of liver, spleen, and brain were determined by plating serial dilutions on TH agar plates. A *p* value less than 0.01 (unpaired *t* test) was considered statistically significant.

## RESULTS

**Identification of the NudP 5'-Nucleotidase in GBS**—Bioinformatics analysis of the NEM316 WT strain genome reveals an uncharacterized gene (systematic name, *gbs1403* or NCBI NP\_735840.1) encoding a putative ectonucleotidase. The corresponding protein was renamed hereafter as NudP following its characterization (see below). *nudP* is a 2073-bp ORF coding for a 690-amino acid polypeptide containing a signal peptide, a putative cell surface localization motif, and the two typical domains of 5'-nucleotidases (Fig. 1A). The amino-terminal region contains the predicted catalytic site within a metallophosphodiesterase motif (metallophosphatase domain (MPP), pfam00149; domain E-value =  $1.1e^{-10}$ ) belonging to a large superfamily of distantly related metallophosphatases (12, 39–41). The NudP carboxyl-terminal motif is typical of the substrate-binding domain of 5'-nucleotidases (pfam02872 domain; E-value =  $4.6e^{-34}$ ) (40–42).

**NudP Is a Mn<sup>2+</sup>-dependent NMP/NDP 5'-Phosphodiesterase**—NudP is a member of a widespread 5'-nucleotidase family (EC 3.1.3.5) found in prokaryotes and eukaryotes that can hydrolyze a wide range of substrates (12). Among these substrates are the phosphoric ester bonds of 5'-tri-, 5'-di-, and 5'-monophosphate nucleoside, nucleic acids, and phosphoproteins (12). More specifically, NudP is related to the *E. coli* UDP-sugar hydrolase (UshA; EC 3.6.1.45) periplasmic 5'-nucleotidase (E-value =  $1e^{-21}$ , 26% identities, 43% similarities on 565 residues), which hydrolyzes 5'-phosphonucleotides and UDP-sugar (42), and to the *S. aureus* AdsA 5'-nucleotidase

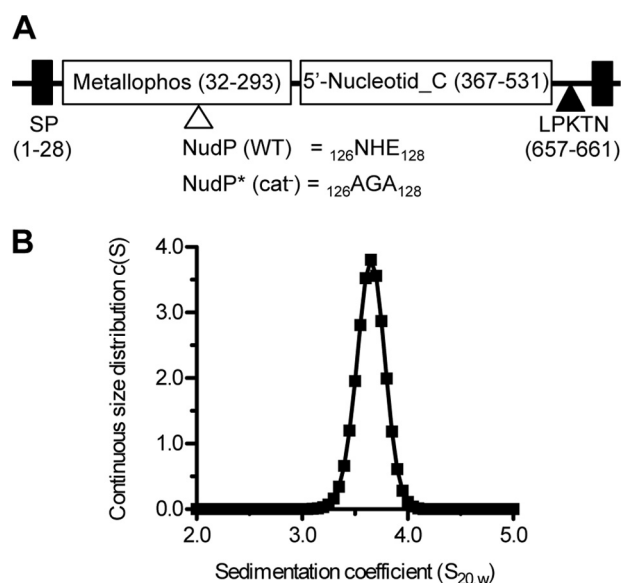


**FIGURE 1. NudP is a monomeric nucleotidase.** *A*, schematic representation of the NudP protein. *White boxes* highlight the two typical domains of 5'-nucleotidases: the metallophosphatase domain (*Metallophos*; residues 32–293, pfam00149) and the substrate-binding domain (*5'-Nucleotid\_C*; residues 367–531, pfam02872). *Filled black boxes* represent the two transmembrane domains (residues 5–27 and 664–683) necessary for secretion (*SP*, signal peptide; residues 1–28) and *LPKTN* cell wall anchoring (*inverted black triangle*; residues 657–661). The position of the conserved NHE motif essential for the stabilization of the transition state of 5'-nucleotidases is highlighted (*white triangle*; residues 126–128) as well as its corresponding mutation to *AGA* in the catalytically inactive (*cat<sup>-</sup>*) mutant *NudP\**. *B*, analytical ultracentrifugation analysis of rNudP. rNudP (residues 28–656) produced and purified from *E. coli* is a monomer with an elongated shape. Sedimentation coefficients are expressed in Svedberg units where  $1\text{ S} = 10^{-13}\text{ s}$ .

( $E$ -value =  $1e^{-13}$ , 23% identities, 40% similarities on 493 residues), which degrades nucleoside mono-, di-, and triphosphates (19).

To characterize its enzymatic activity, we expressed and purified a NudP-truncated form in *E. coli*. rNudP (residues 28–656) contains the metallophosphatase and the substrate-binding domains (Fig. 1*A*) but not the predicted native peptide signal (residues 1–28) or the cell wall anchoring domain (residues 657–690). rNudP was expressed in the *E. coli* periplasm to avoid interference with intracellular metabolism and further purified by osmotic shock followed by ion exchange and gel filtration. rNudP was produced as a soluble protein that migrates between the 58- and 80-kDa molecular mass markers in agreement with its theoretical 68-kDa mass, and its purity estimated by SDS-PAGE was greater than 95% (data not shown). Analytical gel filtration showed that rNudP elutes at a volume similar to aldolase (~158 kDa), suggesting a dimerization and/or an elongated shape. To further characterize rNudP, sedimentation velocity experiments were performed, revealing an  $s_{20,w}$  of 4.0 S, a frictional ratio of 1.4, and a calculated mass of 66 kDa in agreement with an extended monomeric conformation (Fig. 1*B*).

The enzymatic activity of the rNudP protein was tested for a range of substrates and conditions. The optimal enzymatic activity was found to be at pH 7.5, a pH close to that of the blood and body's extracellular fluid, and was dependent on  $\text{Mn}^{2+}$  with an optimum near 5 mM ( $K_m = 2\text{ mM}$ ) (Fig. 2, *A* and *B*). Interestingly, the catalytic activity was low in the presence of  $\text{Ca}^{2+}$  (Fig. 2*B*): a 78% decrease

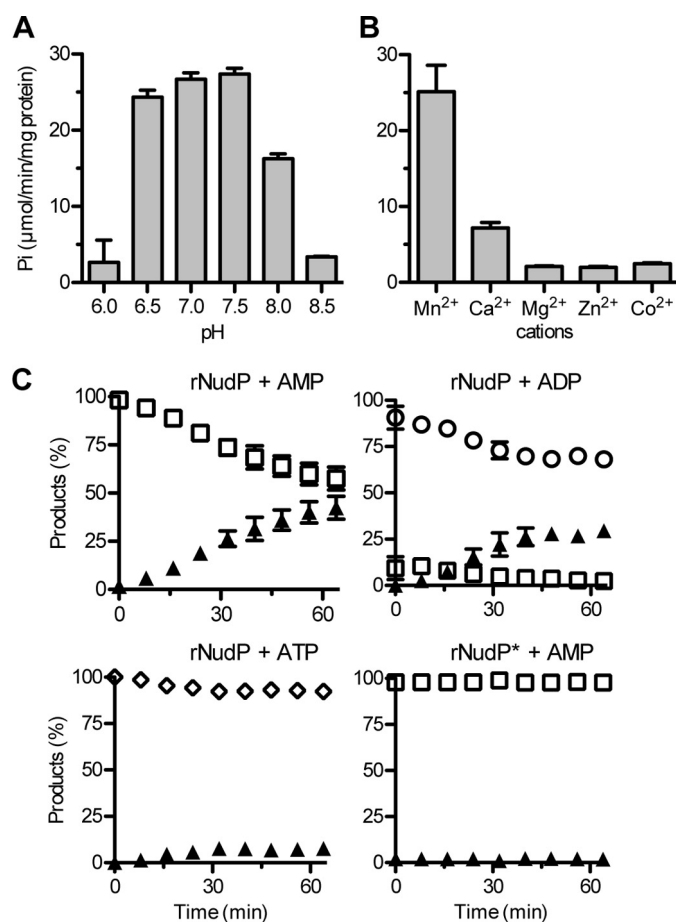


**FIGURE 2. NudP is a manganese-dependent (deoxy)-NMP/NDP 5'-nucleotidase.** *A*, pH optimum for rNudP phosphatase activity. Release of  $\text{P}_i$  by the action of the rNudP protein is optimal at pH 7.5. Quantification of  $\text{P}_i$  was performed with Biomol Green reagents after incubation of 1.5 nM rNudP with 200  $\mu\text{M}$  AMP in the presence of 5 mM  $\text{Mn}^{2+}$  for 30 min. Mean and S.D. (*error bars*) are calculated from three experiments. *B*, effect of cations on rNudP phosphatase activity. The maximal rNudP phosphatase activity is manganese-dependent. Quantification of  $\text{P}_i$  was performed as in *A* except that the pH was fixed to 7.5, and 5 mM concentrations of the different cations were used. rNudP activity is reported as a relative activity ( $=100 \times \text{activity with cation } X / \text{maximal observed activity}$ ). Mean and S.D. (*error bars*) are calculated from three experiments. *C*, kinetic analysis of the rNudP phosphatase activity with AMP, ADP, and ATP as substrates. Experiments were performed at pH 7.5 in the presence of 1.5 nM rNudP, 5 mM  $\text{Mn}^{2+}$ , and 200  $\mu\text{M}$  substrates. Substrate degradation and product formation were followed by rapid resolution HPLC (*filled triangles*, adenosine; *empty squares*, AMP; *empty circles*, ADP; *empty diamonds*, ATP). Inactive rNudP\* with the *AGA* mutation is shown only with AMP. Mean and S.D. (*error bars*) are calculated from at least three independent experiments.

was observed when using 5 mM  $\text{Ca}^{2+}$  instead of 5 mM  $\text{Mn}^{2+}$ ), and it was undetectable (similar to the background level) in the presence of  $\text{Mg}^{2+}$ ,  $\text{Co}^{2+}$ , or  $\text{Zn}^{2+}$  (Fig. 2*B*).

Thus, the kinetic parameters of rNudP were determined in the presence of 5 mM  $\text{Mn}^{2+}$  at pH 7.5 with the different substrates as illustrated in Fig. 2*C* with adenosine nucleotides. The highest NudP specific activities were obtained with ribonucleoside 5'-mono- and -diphosphates but not with the corresponding triphosphates (Table 2). Michaelis constants for AMP, CMP, GMP, and UMP are between 13 and 56  $\mu\text{M}$ , and the  $k_{\text{cat}}/K_m$  values are between  $3 \times 10^4$  and  $1.8 \times 10^5\text{ s}^{-1}\text{ M}^{-1}$  (Table 3). NudP activity was not dependent on the presence of a 2'-hydroxyl group on the ribose moiety, although NudP activ-

## Specific Ecto-5'-nucleosidase Activity of *S. agalactiae*

**TABLE 2**

**Substrate specificities of rNudP**

Reaction velocities were calculated from the initial rates of the release of inorganic phosphate. Reactions were performed in 50 mM Tris, pH 7.5, 5 mM MnCl<sub>2</sub> with 200 μM substrate and 1.5 nM rNudP. Specific activities are expressed in μmol min<sup>-1</sup> mg<sup>-1</sup> of protein, and mean and S.D. are calculated from three experiments. ND, not determined; 2'-dN 3'-MP = 2'-deoxyribonucleoside 3'-monophosphate; A2pA, adenyladenosine monophosphate; Ap3A, diadenosine triphosphate; pNPP, *p*-nitrophenyl phosphate; PRPP, phosphoribosyl pyrophosphate.

	Base			
	A	C	G	U/T
<b>Ribonucleotides</b>				
NTP	<0.1	<0.1	<0.1	<0.1
NDP	9.3 ± 0.6	9.6 ± 2.0	9.8 ± 1.4	12.5 ± 0.9
NMP	21.5 ± 3.2	8.5 ± 1.1	21.9 ± 3.4	21.1 ± 4.0
<b>Deoxyribonucleotides</b>				
dNTP	<0.1	<0.1	<0.1	<0.1
dNDP	5.3 ± 0.4	2.5 ± 0.7	4.5 ± 0.5	1.0 ± 0.5
dNMP	71.8 ± 5.2	64.7 ± 8.0	50.3 ± 4.8	6.9 ± 0.4
2'-dN 3'-MP	ND	ND	<0.1	ND
<b>Sugar nucleotides</b>				
NDP-glucose	ND	ND	1.5 ± 0.6	<0.1
NDP-ribose	3.2 ± 0.9	ND	ND	ND
<b>Miscellaneous</b>				
A2pA, Ap3A, NAD, pNPP, 5'-PRPP	<0.1			

**TABLE 3**

**Kinetic parameters of recombinant rNudP on ribonucleoside 5'-monophosphate**

The  $V_{max}$  and  $K_m$  (mean ± S.D.) were obtained from double reciprocal plots of initial velocity measurements with at least five different concentrations of AMP, CMP, GMP, and UMP. The  $k_{cat}$  (s<sup>-1</sup>) was calculated assuming a molecular mass of 68 kDa.

	$K_m$ μM	$k_{cat}$ s <sup>-1</sup>	$k_{cat}/K_m$ s <sup>-1</sup> M <sup>-1</sup>
AMP	35 ± 8	6.27 ± 0.3	1.8 × 10 <sup>5</sup>
CMP	16 ± 7	0.54 ± 0.03	0.3 × 10 <sup>5</sup>
GMP	56 ± 14	4.36 ± 0.3	0.7 × 10 <sup>5</sup>
UMP	13 ± 7	2.18 ± 0.2	1.6 × 10 <sup>5</sup>

ity was enhanced with dAMP, dCMP, and dGMP as compared with AMP, CMP, and GMP by a factor of 3–10 (see Table 2, Deoxyribonucleotides). In contrast, NudP activity was totally dependent on the presence of a 5'-phosphate on the ribose (Table 2, 2'-deoxyguanosine 3'-monophosphate), and NudP had a low activity on the typical UshA substrate UDP-glucose or other sugar nucleotides (Table 2).

Despite differences in substrate specificities and metal requirement with the *E. coli* UshA and the *S. aureus* AdSA nucleosidases, these enzymes share critical amino acids essential for the stabilization of the transition state. These residues are conserved in NudP (Fig. 1A), suggesting a conserved catalytic mechanism (39–41). To test this hypothesis, the corresponding asparagine (Asn<sup>116</sup>), histidine (His<sup>117</sup>), and glutamic acid (Glu<sup>118</sup>) of NudP were mutated to alanine (Ala<sup>116</sup> and Ala<sup>118</sup>) and glycine (Gly<sup>117</sup>). The resulting recombinant protein, rNudP\*, was inactive whatever the substrates used (Fig. 2C and data not shown).

**NudP Is a Cell Wall-anchored Enzyme Acting on Extracellular Nucleotides**—The GBS strain NEM316 encodes 30 putative cell wall-anchored surface proteins that are covalently attached to the peptidoglycan (32, 38). Cell wall-anchored surface proteins contain a characteristic carboxyl-terminal sorting signal composed of the conserved LPXTG motif followed by a hydrophobic domain and a positively charged tail (43–45). Following

secretion, the sorting signal is cleaved between the threonyl and glycylyl residues of the LPXTG motif, and the threonyl group is covalently attached to the peptidoglycan polymer of the cell wall. The enzyme catalyzing the protease and transpeptidase reactions is a membrane-associated protein called sortase A (SrtA) (38, 43–45).

NudP is one of the two proteins encoded by NEM316 with a degenerated LPXTG motif (Fig. 1A; LPKTN at position 657); the second is the C5a peptidase ScpB (32, 38). To confirm that NudP is anchored to the cell wall, we performed a Western blot analysis of cell wall extracts and concentrated supernatants from NEM316 WT and *srtA*\* mutant strains with polyclonal antibodies made against rNudP. As shown in Fig. 3A, a large amount of NudP was detected in the cell wall extract of the WT strain but not in that of the *srtA*\* mutant. In contrast, we observed that this protein was only present in the culture supernatant of the *srtA*\* mutant and not in that of the WT strain.

To test the consequence of the absence of NudP enzymatic activity, we constructed a GBS mutant expressing an inactive form of NudP. This NudP\* mutant has the same mutations (NHE to AGA) as the rNudP\* inactive form used above (Figs. 1A and 2C). The NudP\* mutant was obtained by mutating the corresponding codons in the chromosome of the WT NEM316 strain in a two-step allelic replacement process. This procedure allowed us to simultaneously select a *nudP*\* mutant and an isogenic strain with a WT *nudP* sequence, referred to hereafter as the WTbk control strain (see “Experimental Procedures”).

The expression and localization of the NudP\* protein were not affected by the mutations introduced in its gene as seen by Western blot analysis (Fig. 3A). Thus, the *nudP*\* mutant expressed an inactive form of NudP at its surface. In addition, cell wall extracts of the WTbk and of the *nudP*\* and *srtA*\* mutants were incubated with AMP, ADP, or ATP in the presence of Mn<sup>2+</sup>. The cell wall extracts of the WTbk, but not of the *nudP*\* and *srtA*\* mutants, hydrolyzed ADP and AMP but not ATP (Fig. 3B and data not shown). Taken together, these results confirm the activity of NudP, its SrtA-dependent cell wall anchoring, and the absence of other cell wall-localized ecto-5'-nucleosidase activity in the tested conditions.

**NudP Catalytic Activity Is Necessary to Escape Blood Clearance and to Colonize Internal Organs**—In the blood, extracellular nucleotides regulate the balance between the pro- and anti-inflammatory responses (1, 2, 8). Therefore, to test the biological function of NudP, we determined the survival of GBS strains in fresh blood of naive mice. For the WTbk bacteria, around 40% of GBS cells were killed within 30–60 min in these conditions (Fig. 4A). The absence of NudP activity increased the bacterial killing rate with only 20% of viable *nudP*\* bacteria, compared with 60% of WTbk bacteria, after 90-min incubation in blood (Fig. 4A). When the blood was supplemented with nucleosides (150 μM adenosine or guanosine), a small but reproducible decrease of bacterial survival was observed (Fig. 4A; 40% viable WTbk bacteria after 60–90-min incubation). Importantly, the increased killing of *nudP*\* compared with the WTbk was abrogated when blood was supplemented with adenosine but not with guanosine, linking the observed phenotype to the absence of NudP enzymatic activity (Fig. 4A).

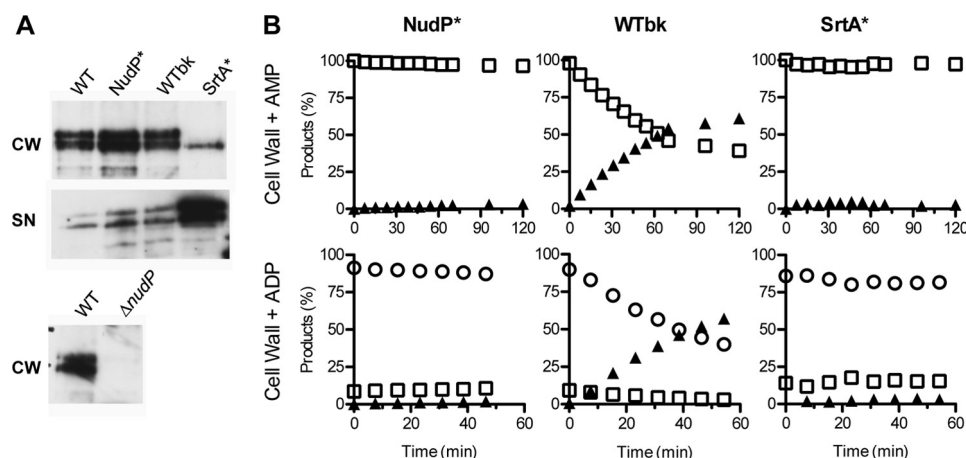


FIGURE 3. **NudP is a cell wall-associated protein acting on extracellular nucleotides.** *A*, immunodetection of NudP by Western analysis of GBS cell wall and secreted proteins. Specific antibodies directed against purified rNudP were used to detect NudP in the cell wall (CW) and in the concentrated culture supernatants (SN) of the NEM316 WT strain, the mutant expressing the inactivated AGA substitution form (NudP\*), the corresponding isogenic complemented strain (WTbk), the inactive SrtA\* mutant, and the *nudP* deletion mutant ( $\Delta nudP$ ). Similar amounts of total cell wall and secreted proteins, corresponding to the extraction from  $10^8$  bacterial cells in midexponential phase in TH broth at 37 °C, were loaded. Shown is a representative experiment of at least three independent experiments. Note that NudP is specifically revealed by two bands migrating closely. As both were absent in the  $\Delta nudP$  extracts, we assume that the smaller band is the result of proteolysis. *B*, kinetic analysis of the cell wall-associated phosphatase activity in the NudP\* mutant, the WTbk complemented strain, and the SrtA\* mutant with AMP and ADP as substrates. Experiments were performed at pH 7.5 in the presence of 0.1  $\mu$ g of cell wall proteins, 5 mM  $Mn^{2+}$ , and 200  $\mu$ M substrates. Substrate degradation and product formation were followed by rapid resolution HPLC (filled triangles, adenosine; empty squares, AMP; empty circles, ADP).

Because the *nudP*\* mutant was killed more efficiently by blood cells *in vitro*, we tested its *in vivo* virulence in two models of infection. First, 3-day-old neonate rats were infected with  $5 \times 10^6$  bacteria by intraperitoneal injections. Although all animals died within 3 days upon infection with the WTbk control strain, the absence of NudP activity was associated with a 50% decrease in overall mortality (Fig. 4*B*). In a second experiment, BALB/c mice were infected intravenously with  $5 \times 10^7$  bacteria, and blood and organ (brain, liver, and spleen) colonization was monitored at 24 and 48 h postinfection. At 24 h, no significant differences were observed between the WTbk and the NudP\* mutant (Fig. 4*C*) even in the blood where an increased killing of the *nudP*\* mutant was observed *in vitro* (Fig. 4*A*). However, 48 h postinfection, a higher number (>1 log) of viable bacteria were recovered in all tested organs of mice infected with the WTbk control strain compared with those infected with the *nudP*\* mutant (Fig. 4*A*). Overall, these *in vivo* experiments highlight the importance of NudP for bacterial virulence and organ colonization.

## DISCUSSION

The main GBS virulence-associated factors identified to date are secreted and surface-exposed molecules (*e.g.* capsule, hemolysin, lipoproteins, and cell wall-associated proteins) that mediate interactions with host cells (46–50). Among the 30 GBS proteins covalently linked to the cell wall by an LPXTG-type motif (32), several are directly involved in GBS virulence, such as adhesins and immunomodulators (37, 38, 48, 49). In this study, we report the enzymatic activity of a previously uncharacterized cell wall protein of GBS and its function during pathogenesis in animal models of infection. Although NudP has an imperfect LPXTG motif (the terminal glycine is replaced by an asparagine residue), a sequence also found in the C5a peptidase ScpB (32, 38), we observed that NudP is mainly associated to the cell wall by a mechanism dependent on the sortase A enzyme

(43–45). This extracellular localization and the biochemical characterization of the recombinant protein demonstrate that NudP belongs to the ecto-5'-nucleotidase (eN) enzyme family (12). Its specificity is unusual for an eN because it hydrolyzes NMP and NDP but not NTPs and specifically requires  $Mn^{2+}$  cations for its activity. This is in marked contrast with human ectonucleotidases, which are divided into two major groups: the eN and the NTPDase enzyme families (12). In mammals, these two unrelated enzyme families act sequentially to hydrolyze tri- and diphosphate nucleosides (mostly by the CD39/NTPDase1 enzyme) and monophosphate nucleosides (mostly by the CD73/eN enzyme). Thus, NudP is clearly an eN enzyme characterized by the metallophosphatase and nucleotide-binding domains but shares some substrate specificity with NTPDase (12).

Interestingly, the apyrase conserved regions corresponding to the active domain of NTPDase are almost ubiquitous in eukaryotes and absent in prokaryotes except *Legionella pneumophila* (15, 16). In contrast, eNs are widespread in bacteria, but only a few of them have been characterized. The homology between bacterial and eukaryotic 5'-nucleotidases is low, but the domain organization and the key residues for catalytic activity are conserved (39). The periplasmic *E. coli* UshA protein was the first bacterial 5'-nucleotidase characterized. UshA hydrolyzes UDP-glucose and other nucleotide diphosphate sugars to produce sugar 1-phosphate. The main function of UshA was therefore proposed to be as a metabolic enzyme. Thereafter, it was demonstrated that NTP, NDP, NMP, and nucleotide sugars were also UshA substrates, but the biological function of this enzyme remains unclear (39, 42).

More recently, ecto-5'-nucleotidases in bacterial pathogens have been identified, including the *S. aureus* AdsA enzyme (18–20). AdsA was first described as an adenosine synthase because of its ability to hydrolyze AMP into adenosine (18),

## Specific Ecto-5'-nucleosidase Activity of *S. agalactiae*

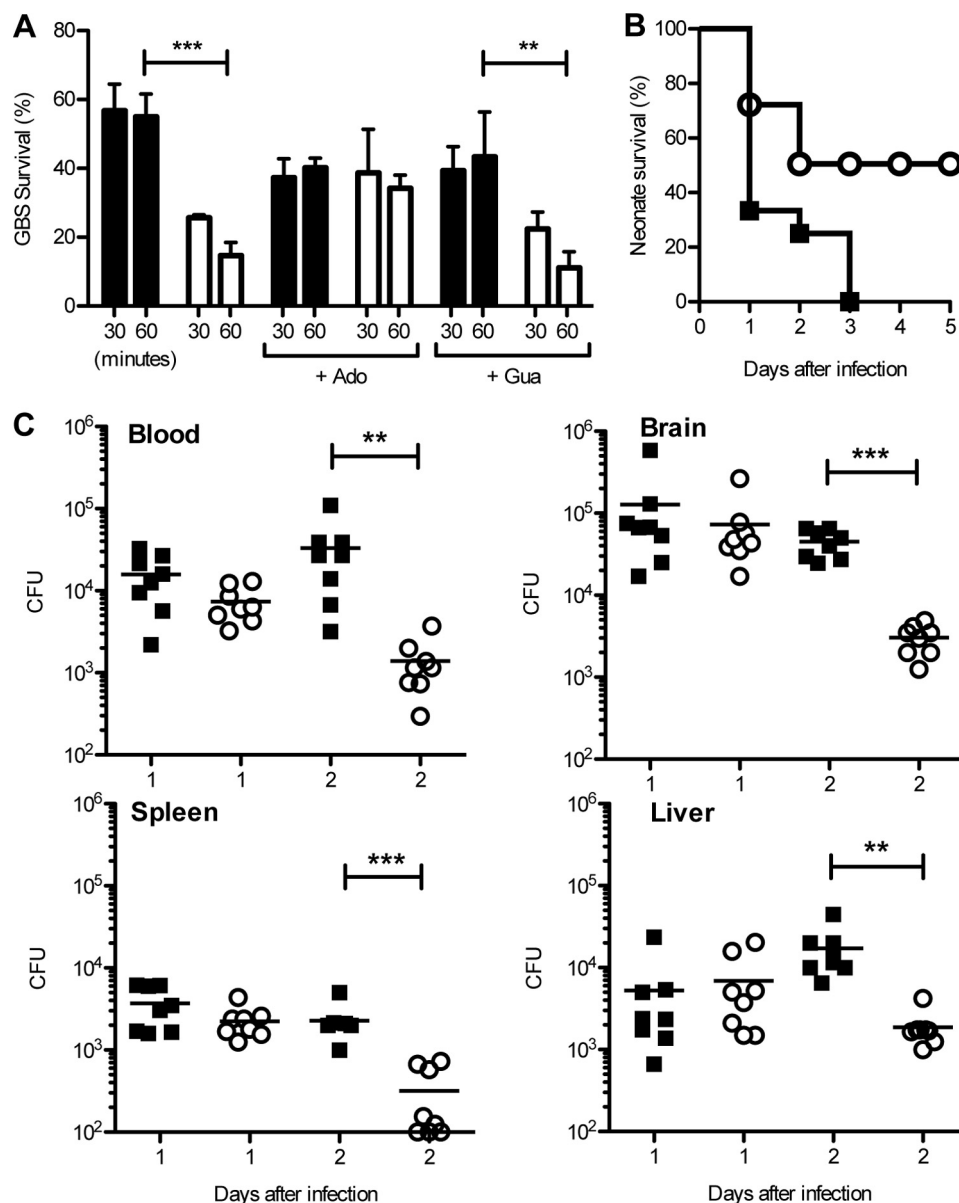


**FIGURE 4. The NudP enzymatic activity contributes to GBS survival in blood and colonization of internal organs.** A, NudP contributes to GBS survival in blood.  $5 \times 10^7$  bacterial cells of the *nudP\** mutant (white bars) or the isogenic WTbk complemented strain (black bars) were incubated at 37 °C with fresh blood of BALB/c mice supplemented with 150  $\mu$ M adenosine (+ Ado) or guanosine (+ Gua). Aliquots were taken at the indicated time points (30 and 60 min), and bacterial survival was calculated after 24-h incubation on an agar plate as the total number of cfu at a given time versus the number of cfu at time 0. Mean and S.D. (error bars) are calculated from two independent experiments in duplicate, and statistical significance is indicated by asterisks (unpaired *t* test; \*\*\*,  $p < 0.001$ ; \*\*,  $p < 0.01$ ). B, NudP contributes to GBS virulence in neonate animals.  $5 \times 10^6$  bacterial cells of the *nudP\** mutant (empty circles) or the isogenic WTbk complemented strain (filled squares) were inoculated intraperitoneally into 2-day-old neonatal Sprague-Dawley rats. Animal survival was followed for 5 days, and the mortality curve is the result of two independent experiments with  $2 \times 10$  animals inoculated with bacterial strains. C, NudP contributes to colonization of internal organs.  $5 \times 10^7$  bacterial cells of the *nudP\** mutant (empty circles) or the isogenic WTbk complemented strain (filled squares) were injected intravenously into 5-week-old BALB/c mice. At 24 and 48 h postinfection, groups of eight mice were sacrificed, and organ colonization was quantified by cfu counting. One representative experiment is shown with statistical significance indicated by asterisks (unpaired *t* test; \*\*\*,  $p < 0.001$ ; \*\*,  $p < 0.01$ ).

whereas further characterization demonstrated that AdsA is an eN enzyme that also hydrolyzes ADP, ATP, GTP, GDP, and GMP as well as 2'-deoxyadenosine 3'-monophosphate (19, 20). Homologues of ecto-5'-nucleotidases are present in several Gram-positive pathogens, including *Enterococcus faecalis*, *Bacillus anthracis*, *Listeria monocytogenes*, *Streptococcus pyogenes* (18), and *Streptococcus sanguinis* (21) but absent in the related human pathogen *Streptococcus pneumoniae*.<sup>3</sup>

A similarity search or pairwise comparison is not effective to predict the biochemical function of bacterial ecto-5'-nucleotidases. Indeed, a BlastP search indicates that NudP is more similar to *E. coli* UshA than to *S. aureus* AdsA protein. However, these homologies are restricted to key amino acid clusters as observed previously by comparing bacterial and eukaryotic enzymes (12, 39). On the other hand, regions and residues critical for substrate specificity and metal coordination are less conserved, suggesting a specific adaptation of each enzyme. For instance, NudP does not hydrolyze triphosphorylated nucleo-

<sup>3</sup> A. Firon and P. Trieu-Cuot, unpublished observation.

sides and specifically requires  $Mn^{2+}$ . In contrast, AdSA ( $Mn^{2+}$  or  $Mg^{2+}$ ) and UshA ( $Mn^{2+}$  or  $Mg^{2+}$ ; stimulated by  $Co^{2+}$ ) display different cofactor specificities and are able to hydrolyze these substrates. In addition, NudP has a more restricted pH range of activity (between 6.5 and 7.5) than AdSA (between 4 and 10) (19). Despite these differences, these enzymes share a common catalytic mechanism. Structure-function analysis of the *E. coli* 5'-nucleotidase provided the first insights into substrate binding and catalysis. Among the residues conserved in ectonucleotidases, Asn<sup>116</sup> and His<sup>218</sup> were shown to be involved in the stabilization of the transition state, and mutation of His<sup>117</sup> to Asn diminishes the activity to 0.04% of the wild-type level (12, 40). The absence of catalytic activity of the NudP\* form with an AGA substitution of the NHE motif supports this model.

By analyzing the NudP\* inactive mutant, we found that this enzymatic activity is necessary for GBS survival in blood and contributes to organ colonization in animal models of infection. In particular, we observed that the increased killing of the NudP\* mutant in blood compared with the WT strain was abolished when an exogenous supply of adenosine was provided. However, when tested *in vivo* in adult animals after intravenous injections, the number of NudP\* mutant cfu in blood was similar to that in the WT strain 24 h after the infection. The NudP\* defects in blood and organs appeared only at the later time point of 48 h, suggesting that NudP is dispensable at early time points of infection. Because NudP acts on extracellular nucleotides, it highlights the role of these extracellular nucleotides in modulating host responses to bacterial infections (2, 8, 14, 18, 51).

The immune cells and signaling pathways affected by extracellular nucleotides during GBS infections remain to be determined. The function and the subversion of the eATP receptors, the P2X family, during infections are mainly documented for intracellular microbial pathogens (14, 51). In contrast, few studies have addressed the function of eATP/eAdo receptors during infections by extracellular pathogens and hence the biological consequences of modulating the eATP/eADP ratio (14, 51). In mammals, the two main ectonucleotidases, CD39 and CD73, expressed at the surface of immune cells control the eATP/eAdo ratio, and their inactivation is detrimental to the clearance of polymicrobial infections (13, 52). This eATP/eAdo ratio serves as a central hub to control the balance between pro- and anti-inflammatory responses. However, P2X receptors and eATP are dispensable in macrophages for caspase-1 activation by *S. pyogenes* (53). As this bacterium encodes a yet-to-be-characterized NudP homologue, it is likely that the involvement of extracellular nucleotides in controlling other signaling pathways is underestimated. In *S. aureus*, it was proposed that the main activity of the AdSA ectonucleotidase is to synthesize adenosine to dampen the proinflammatory response mediated by neutrophils (18) and very recently to inhibit macrophage recruitment and promote immune cell apoptosis following synthesis of deoxyadenosine (20). These multiple tasks of AdSA might be due to the pleiotropic function of extracellular nucleotides in cell signaling (1, 2, 9–11). A key difference between the *S. aureus* AdSA and the *S. agalactiae* NudP, apart from the pH range and the metal requirement, is the inability of NudP to

hydrolyze deoxynucleoside 3'-phosphate. Therefore, although the two bacterial species secrete a nuclease involved in neutrophil extracellular trap degradation (20, 54), the deoxyadenosine 3'-phosphate resulting from DNA degradation can be used as a substrate by AdSA but not by NudP.

In conclusion, our study on NudP highlights the diversity of enzymatic reactions performed by a widespread enzyme family and suggests that this diversity might be related to the adaptation of a given organism to specific hosts or environmental niches. Deciphering the precise mechanism(s) and consequence(s) of GBS manipulation of extracellular nucleotides might help to understand and control infections caused by this extracellular pathogen.

*Acknowledgments*—We thank Stina Linden and Nina Grau for contributions to the work during Master courses. We also thank Shaynoor Dramsi for constructive discussions in the course of this work.

## REFERENCES

- Eltzschig, H. K., Sitkovsky, M. V., and Robson, S. C. (2012) Purinergic signaling during inflammation. *N. Engl. J. Med.* **367**, 2322–2333
- Junger, W. G. (2011) Immune cell regulation by autocrine purinergic signalling. *Nat. Rev. Immunol.* **11**, 201–212
- Elliott, M. R., Chekeni, F. B., Trampont, P. C., Lazarowski, E. R., Kadl, A., Walk, S. F., Park, D., Woodson, R. I., Ostankovich, M., Sharma, P., Lysiak, J. J., Harden, T. K., Leitinger, N., and Ravichandran, K. S. (2009) Nucleotides released by apoptotic cells act as a find-me signal to promote phagocytic clearance. *Nature* **461**, 282–286
- Piccini, A., Carta, S., Tassi, S., Lasiglié, D., Fossati, G., and Rubartelli, A. (2008) ATP is released by monocytes stimulated with pathogen-sensing receptor ligands and induces IL-1 $\beta$  and IL-18 secretion in an autocrine way. *Proc. Natl. Acad. Sci. U.S.A.* **105**, 8067–8072
- Chen, Y., Corriden, R., Inoue, Y., Yip, L., Hashiguchi, N., Zinkernagel, A., Nizet, V., Insel, P. A., and Junger, W. G. (2006) ATP release guides neutrophil chemotaxis via P2Y2 and A3 receptors. *Science* **314**, 1792–1795
- Yip, L., Woehrle, T., Corriden, R., Hirsh, M., Chen, Y., Inoue, Y., Ferrari, V., Insel, P. A., and Junger, W. G. (2009) Autocrine regulation of T-cell activation by ATP release and P2X7 receptors. *FASEB J.* **23**, 1685–1693
- Trautmann, A. (2009) Extracellular ATP in the immune system: more than just a “danger signal”. *Sci. Signal.* **2**, pe6
- Vitiello, L., Gorini, S., Rosano, G., and la Sala, A. (2012) Immunoregulation through extracellular nucleotides. *Blood* **120**, 511–518
- Haskó, G., Linden, J., Cronstein, B., and Pacher, P. (2008) Adenosine receptors: therapeutic aspects for inflammatory and immune diseases. *Nat. Rev. Drug Discov.* **7**, 759–770
- Sitkovsky, M. V., and Ohta, A. (2005) The ‘danger’ sensors that STOP the immune response: the A2 adenosine receptors? *Trends Immunol.* **26**, 299–304
- Khakh, B. S., and North, R. A. (2006) P2X receptors as cell-surface ATP sensors in health and disease. *Nature* **442**, 527–532
- Zimmermann, H., Zebisch, M., and Sträter, N. (2012) Cellular function and molecular structure of ecto-nucleotidases. *Purinergic Signal.* **8**, 437–502
- Deaglio, S., Dwyer, K. M., Gao, W., Friedman, D., Usheva, A., Erat, A., Chen, J. F., Enyoloji, K., Linden, J., Oukka, M., Kuchroo, V. K., Strom, T. B., and Robson, S. C. (2007) Adenosine generation catalyzed by CD39 and CD73 expressed on regulatory T cells mediates immune suppression. *J. Exp. Med.* **204**, 1257–1265
- Sansom, F. M., Robson, S. C., and Hartland, E. L. (2008) Possible effects of microbial ecto-nucleoside triphosphate diphosphohydrolases on host-pathogen interactions. *Microbiol. Mol. Biol. Rev.* **72**, 765–781
- Sansom, F. M., Newton, H. J., Crikis, S., Cianciotto, N. P., Cowan, P. J., d’Apice, A. J., and Hartland, E. L. (2007) A bacterial ecto-triphosphate

## Specific Ecto-5'-nucleosidase Activity of *S. agalactiae*

- diphosphohydrolase similar to human CD39 is essential for intracellular multiplication of *Legionella pneumophila*. *Cell. Microbiol.* **9**, 1922–1935
16. Sansom, F. M., Riedmaier, P., Newton, H. J., Dunstone, M. A., Müller, C. E., Stephan, H., Byres, E., Beddoe, T., Rossjohn, J., Cowan, P. J., d'Apice, A. J., Robson, S. C., and Hartland, E. L. (2008) Enzymatic properties of an ecto-nucleoside triphosphate diphosphohydrolase from *Legionella pneumophila*: substrate specificity and requirement for virulence. *J. Biol. Chem.* **283**, 12909–12918
  17. Vivian, J. P., Riedmaier, P., Ge, H., Le Nours, J., Sansom, F. M., Wilce, M. C., Byres, E., Dias, M., Schmidberger, J. W., Cowan, P. J., d'Apice, A. J., Hartland, E. L., Rossjohn, J., and Beddoe, T. (2010) Crystal structure of a *Legionella pneumophila* ecto-triphosphate diphosphohydrolase, a structural and functional homolog of the eukaryotic NTPDases. *Structure* **18**, 228–238
  18. Thammavongsa, V., Kern, J. W., Missiakas, D. M., and Schneewind, O. (2009) *Staphylococcus aureus* synthesizes adenosine to escape host immune responses. *J. Exp. Med.* **206**, 2417–2427
  19. Thammavongsa, V., Schneewind, O., and Missiakas, D. M. (2011) Enzymatic properties of *Staphylococcus aureus* adenosine synthase (AdsA). *BMC Biochem.* **12**, 56
  20. Thammavongsa, V., Missiakas, D. M., and Schneewind, O. (2013) *Staphylococcus aureus* degrades neutrophil extracellular traps to promote immune cell death. *Science* **342**, 863–866
  21. Fan, J., Zhang, Y., Chuang-Smith, O. N., Frank, K. L., Guenther, B. D., Kern, M., Schlievert, P. M., and Herzberg, M. C. (2012) Ecto-5'-nucleotidase: a candidate virulence factor in *Streptococcus sanguinis* experimental endocarditis. *PLoS One* **7**, e38059
  22. Johri, A. K., Paoletti, L. C., Glaser, P., Dua, M., Sharma, P. K., Grandi, G., and Rappuoli, R. (2006) Group B *Streptococcus*: global incidence and vaccine development. *Nat. Rev. Microbiol.* **4**, 932–942
  23. Thigpen, M. C., Whitney, C. G., Messonnier, N. E., Zell, E. R., Lynfield, R., Hadler, J. L., Harrison, L. H., Farley, M. M., Reingold, A., Bennett, N. M., Craig, A. S., Schaffner, W., Thomas, A., Lewis, M. M., Scallan, E., and Schuchat, A. (2011) Bacterial meningitis in the United States, 1998–2007. *N. Engl. J. Med.* **364**, 2016–2025
  24. Edmond, K. M., Kortsalioudaki, C., Scott, S., Schrag, S. J., Zaidi, A. K., Cousens, S., and Heath, P. T. (2012) Group B streptococcal disease in infants aged younger than 3 months: systematic review and meta-analysis. *Lancet* **379**, 547–556
  25. Verani, J. R., McGee, L., and Schrag, S. J. (2010) Prevention of perinatal group B streptococcal disease—revised guidelines from CDC, 2010. *MMWR Recomm. Rep.* **59**, 1–36
  26. Henneke, P., and Berner, R. (2006) Interaction of neonatal phagocytes with group B streptococcus: recognition and response. *Infect. Immun.* **74**, 3085–3095
  27. Levy, O. (2007) Innate immunity of the newborn: basic mechanisms and clinical correlates. *Nat. Rev. Immunol.* **7**, 379–390
  28. Kollmann, T. R., Levy, O., Montgomery, R. R., and Goriely, S. (2012) Innate immune function by Toll-like receptors: distinct responses in newborns and the elderly. *Immunity* **37**, 771–783
  29. Levy, O., Coughlin, M., Cronstein, B. N., Roy, R. M., Desai, A., and Wesels, M. R. (2006) The adenosine system selectively inhibits TLR-mediated TNF- $\alpha$  production in the human newborn. *J. Immunol.* **177**, 1956–1966
  30. Pettengill, M., Robson, S., Tresenrieter, M., Millán, J. L., Usheva, A., Bingham, T., Belderbos, M., Bergelson, I., Burl, S., Kampmann, B., Gelinias, L., Kollmann, T., Bont, L., and Levy, O. (2013) Soluble ecto-5'-nucleotidase (5'-NT), alkaline phosphatase, and adenosine deaminase (ADA1) activities in neonatal blood favor elevated extracellular adenosine. *J. Biol. Chem.* **288**, 27315–27326
  31. Trigo, G., Ferreira, P., Ribeiro, N., Dinis, M., Andrade, E. B., Melo-Cristino, J., Ramirez, M., and Tavares, D. (2008) Identification of immunoreactive extracellular proteins of *Streptococcus agalactiae* in bovine mastitis. *Can. J. Microbiol.* **54**, 899–905
  32. Glaser, P., Rusniok, C., Buchrieser, C., Chevalier, F., Frangeul, L., Msadek, T., Zouine, M., Couvé, E., Lalioui, L., Poyart, C., Trieu-Cuot, P., and Kunst, F. (2002) Genome sequence of *Streptococcus agalactiae*, a pathogen causing invasive neonatal disease. *Mol. Microbiol.* **45**, 1499–1513
  33. Betton, J. M., and Hofnung, M. (1996) Folding of a mutant maltose-binding protein of *Escherichia coli* which forms inclusion bodies. *J. Biol. Chem.* **271**, 8046–8052
  34. Schuck, P. (2000) Size-distribution analysis of macromolecules by sedimentation velocity ultracentrifugation and Lamm equation modeling. *Biophys. J.* **78**, 1606–1619
  35. Heckman, K. L., and Pease, L. R. (2007) Gene splicing and mutagenesis by PCR-driven overlap extension. *Nat. Protoc.* **2**, 924–932
  36. Firon, A., Tazi, A., Da Cunha, V., Brinster, S., Sauvage, E., Dramsi, S., Golenbock, D. T., Glaser, P., Poyart, C., and Trieu-Cuot, P. (2013) The Abi-domain protein Abx1 interacts with the CovS histidine kinase to control virulence gene expression in group B *Streptococcus*. *PLoS Pathog.* **9**, e1003179
  37. Konto-Ghiorgi, Y., Mairey, E., Mallet, A., Duménil, G., Caliot, E., Trieu-Cuot, P., and Dramsi, S. (2009) Dual role for pilus in adherence to epithelial cells and biofilm formation in *Streptococcus agalactiae*. *PLoS Pathog.* **5**, e1000422
  38. Lalioui, L., Pellegrini, E., Dramsi, S., Baptista, M., Bourgeois, N., Doucet-Populaire, F., Rusniok, C., Zouine, M., Glaser, P., Kunst, F., Poyart, C., and Trieu-Cuot, P. (2005) The SrtA sortase of *Streptococcus agalactiae* is required for cell wall anchoring of proteins containing the LPXTG motif, for adhesion to epithelial cells, and for colonization of the mouse intestine. *Infect. Immun.* **73**, 3342–3350
  39. Knöfel, T., and Sträter, N. (1999) X-ray structure of the *Escherichia coli* periplasmic 5'-nucleotidase containing a dimetal catalytic site. *Nat. Struct. Biol.* **6**, 448–453
  40. Knöfel, T., and Sträter, N. (2001) *E. coli* 5'-nucleotidase undergoes a hinge-bending domain rotation resembling a ball-and-socket motion. *J. Mol. Biol.* **309**, 255–266
  41. Knöfel, T., and Sträter, N. (2001) Mechanism of hydrolysis of phosphate esters by the dimetal center of 5'-nucleotidase based on crystal structures. *J. Mol. Biol.* **309**, 239–254
  42. Krug, U., Patzschke, R., Zebisch, M., Balbach, J., and Sträter, N. (2013) Contribution of the two domains of *E. coli* 5'-nucleotidase to substrate specificity and catalysis. *FEBS Lett.* **587**, 460–466
  43. Dramsi, S., Trieu-Cuot, P., and Bierre, H. (2005) Sorting sortases: a nomenclature proposal for the various sortases of Gram-positive bacteria. *Res. Microbiol.* **156**, 289–297
  44. Marraffini, L. A., Dedent, A. C., and Schneewind, O. (2006) Sortases and the art of anchoring proteins to the envelopes of Gram-positive bacteria. *Microbiol. Mol. Biol. Rev.* **70**, 192–221
  45. Hendrickx, A. P., Budzik, J. M., Oh, S. Y., and Schneewind, O. (2011) Architects at the bacterial surface—sortases and the assembly of pili with isopeptide bonds. *Nat. Rev. Microbiol.* **9**, 166–176
  46. Lindahl, G., Ståhlhammar-Carlemalm, M., and Areschoug, T. (2005) Surface proteins of *Streptococcus agalactiae* and related proteins in other bacterial pathogens. *Clin. Microbiol. Rev.* **18**, 102–127
  47. Henneke, P., Dramsi, S., Mancuso, G., Chraïbi, K., Pellegrini, E., Theilacker, C., Hübner, J., Santos-Sierra, S., Teti, G., Golenbock, D. T., Poyart, C., and Trieu-Cuot, P. (2008) Lipoproteins are critical TLR2 activating toxins in group B streptococcal sepsis. *J. Immunol.* **180**, 6149–6158
  48. Nobbs, A. H., Lamont, R. J., and Jenkinson, H. F. (2009) *Streptococcus* adherence and colonization. *Microbiol. Mol. Biol. Rev.* **73**, 407–450
  49. Tazi, A., Disson, O., Bellais, S., Bouaboud, A., Dmytruk, N., Dramsi, S., Mistou, M. Y., Khun, H., Mechler, C., Tardieux, I., Trieu-Cuot, P., Lecuit, M., and Poyart, C. (2010) The surface protein HvgA mediates group B streptococcus hypervirulence and meningeal tropism in neonates. *J. Exp. Med.* **207**, 2313–2322
  50. Whidbey, C., Harrell, M. I., Burnside, K., Ngo, L., Becraft, A. K., Iyer, L. M., Aravind, L., Hitti, J., Waldorf, K. M., and Rajagopal, L. (2013) A hemolytic pigment of group B *Streptococcus* allows bacterial penetration of human placenta. *J. Exp. Med.* **210**, 1265–1281
  51. Miller, C. M., Boulter, N. R., Fuller, S. J., Zakrzewski, A. M., Lees, M. P., Saunders, B. M., Wiley, J. S., and Smith, N. C. (2011) The role of the P2X receptor in infectious diseases. *PLoS Pathog.* **7**, e1002212
  52. Haskó, G., Csóka, B., Koscsó, B., Chandra, R., Pacher, P., Thompson, L. F., Deitch, E. A., Spolarics, Z., Virág, L., Gergely, P., Rolandelli, R. H., and Németh, Z. H. (2011) Ecto-5'-nucleotidase (CD73) decreases mortality

- and organ injury in sepsis. *J. Immunol.* **187**, 4256–4267
53. Harder, J., Franchi, L., Muñoz-Planillo, R., Park, J. H., Reimer, T., and Núñez, G. (2009) Activation of the Nlrp3 inflammasome by *Streptococcus pyogenes* requires streptolysin O and NF- $\kappa$ B activation but proceeds independently of TLR signaling and P2X7 receptor. *J. Immunol.* **183**, 5823–5829
54. Derré-Bobillot, A., Cortes-Perez, N. G., Yamamoto, Y., Kharrat, P., Couvé, E., Da Cunha, V., Decker, P., Boissier, M. C., Escartin, F., Cesselin, B., Langella, P., Bermúdez-Humarán, L. G., and Gaudu, P. (2013) Nuclease A (Gbs0661), an extracellular nuclease of *Streptococcus agalactiae*, attacks the neutrophil extracellular traps and is needed for full virulence. *Mol. Microbiol.* **89**, 518–531

**Extracellular Nucleotide Catabolism by the Group B *Streptococcus*  
Ectonucleotidase NudP Increases Bacterial Survival in Blood**  
Arnaud Firon, Marcia Dinis, Bertrand Raynal, Claire Poyart, Patrick Trieu-Cuot and  
Pierre Alexandre Kaminski

*J. Biol. Chem.* 2014, 289:5479-5489.

doi: 10.1074/jbc.M113.545632 originally published online January 15, 2014

---

Access the most updated version of this article at doi: [10.1074/jbc.M113.545632](https://doi.org/10.1074/jbc.M113.545632)

Alerts:

- [When this article is cited](#)
- [When a correction for this article is posted](#)

[Click here](#) to choose from all of JBC's e-mail alerts

This article cites 54 references, 23 of which can be accessed free at  
<http://www.jbc.org/content/289/9/5479.full.html#ref-list-1>